Experimental evidence for the key role of the ion heat channel in the physics of the L-H transition

F. Ryter, L. Barrera Orte, B. Kurzan, R.M. McDermott, G. Tardini, E. Viezzer,
M. Bernert, R. Fischer and the ASDEX Upgrade Team
Max-Planck-Institut für Plasmaphysik, D-85748 Garching

1. Introduction

Presently, the most favored paradigm to explain the transition from L to H mode is based on turbulence reduction induced by $E \times B$ shear flow, [1]. In the narrow region at the very edge of the plasma, the E_r profile exhibits a clear negative well such that ∇E_r induces a perpendicular sheared flow which stabilizes the turbulence, as confirmed experimentally, [2, 3, 4]. The E_r well is weakly pronounced in L-mode, much deeper in H-mode, while it takes intermediate values just before the L-H transition, [5]. It has been shown that the edge E_r is essentially induced by the main ions according to neoclassical theory, [6], and therefore mainly determined by the gradient of the main ion pressure, $E_r = \nabla p_i/(e \cdot n_i)$, where n_i is the ion density and e the elementary charge, [7, 8, 9]. This strongly suggests that the ion heat flux at the plasma edge might be a key player in the L-H transition through its impact on ∇p_i. This is indeed demonstrated by the experimental study carried out in the ASDEX Upgrade tokamak, presented here and in more details in [10], from which the figures shown here are adapted.

This analysis is only possible if the electron and ion heat fluxes can be separated up to the plasma edge, at the L-H transition. This condition is only fulfilled at rather low density where the collisional electron-ion energy exchange, $p_{ei} \propto n_e n_i (T_e - T_i)/T_e^{3/2}$, is well defined. Note that p_{ei} strongly increases with density, but saturates and decreases at high T_e. In our experiment we mainly use ECRH which provides pure electron heating and a clear difference between T_e and T_i, ($T_e > T_i$). A few discharges have been performed with NBI at very low acceleration voltage which provide dominant ion heating yielding $T_e < T_i$. The heat fluxes are provided by time-dependent power balance analyses with the TRANSP code, [11]. The edge heat fluxes used here are the surface integrated values, $Q_{i,edge}$ and $Q_{e,edge}$, taken at $\rho_{tor} = 0.95$. They are in MW and can be directly compared to the power threshold. The required profiles are yielded by the standard diagnostics available at ASDEX Upgrade, whereby it should be pointed out that T_i and plasma rotation can be measured in ECRH heated discharges using NBI blips of about 10 ms of duration, [12].

2. L-H transitions with ECRH

We first focus on L-H transitions obtained with ECRH in which the only source of ion heating is provided by p_{ei}. The L-H power threshold, P_{L-H}, is well-known to be non-monotonic with a minimum and clear increase towards low density, [13] for ASDEX Upgrade, where a dependence of P_{L-H} on plasma current (I_p) has also been found recently, [14]. The electron and ion heat fluxes can only be separated correctly in the low density branch.

The results are presented in figure 1 (a) where P_{L-H} and $Q_{i,edge}$ are plotted versus density. The P_{L-H} points decrease with increasing density, as well-known for this density region, but, in contrast, $Q_{i,edge}^{L-H}$ increases linearly with density, as underlined by the fit $Q_{i,edge}^{L-H,fit} = 0.18\bar{n}_e$.

Note the very large difference between $Q_{i,edge}^{L-H}$ and P_{L-H} in this density range, due to the small values of p_{ei} at these low densities. It should be emphasized that the different P_{L-H} values found at different plasma current in the low density range are not reflected by $Q_{i,edge}^{L-H}$ which exhibit the same values at 1 MA and 0.6 MA.

The transport analysis reveals that this effect is caused by the confinement dependence on I_p such that, for a given heating power, T_e is lower but p_{ei} higher at 0.6 MA than at 1 MA.

In contrast, the electron heat flux for the same dataset (not shown) does not exhibit any coherent pattern: it mainly follows the trends of P_{L-H} and the values depend on I_p. This indicates that this $Q_{e,edge}$ plays a minor role in the L-H transition physics, while the coherence of $Q_{i,edge}$ strongly suggests that it is a major player, as expected from the physics picture described in the introduction.

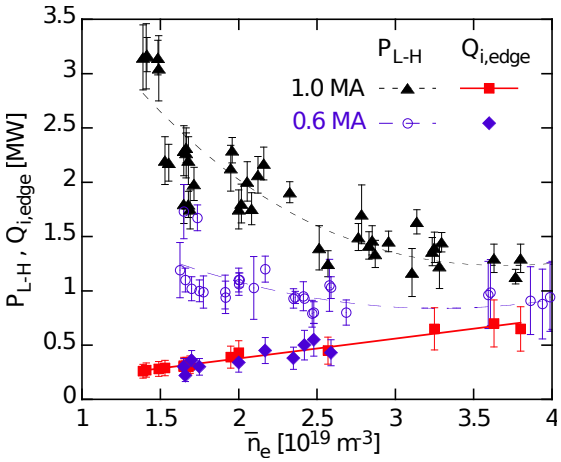

Figure 1: *L-H transitions with ECRH: Power threshold and edge ion heat flux versus line-averaged density at the L-H transition for 1 MA and 0.6 MA discharges. The lines are fits.*

The H-L back transition has also been studied and P_{H-L} was found to be very similar to P_{L-H}, [14]. For 13 cases we could calculate $Q_{i,edge}^{H-L}$ which is found to be very similar to $Q_{i,edge}^{L-H}$: it exhibits the same density dependence and also unifies the points at different current. There is no clear sign of a hysteresis. Here also $Q_{e,edge}^{H-L}$ does not exhibit any coherent pattern.

The main properties of the electron-ion collisional coupling, T_e dependence and increase with density, can be assessed in the experiments. This is illustrated by a data set of L-mode and L-H points in a density range 1.4 - 1.7 10^{19}m^{-3}, at different values of P_{ECRH}. Figure 2 shows $Q_{i,edge}$ plotted versus density. These points confirm that no H-mode occurs below $Q_{i,edge}^{L-H,fit}$. A dedicated density scan at constant heating power marked with blue symbols indicates how $Q_{i,edge}$ increases with density and that the L-H transition occurs exactly at the value of $Q_{i,edge}^{L-H}$ obtained by increasing the heating power. This is a further strong indication that the edge ion heat flux is a key player. Finally, L-mode points at very low density and high P_{ECRH} are also reported (violet triangles). In these discharges no transition to H-mode occurred because the maximum reachable value of $Q_{i,edge}$ was not sufficient to induce

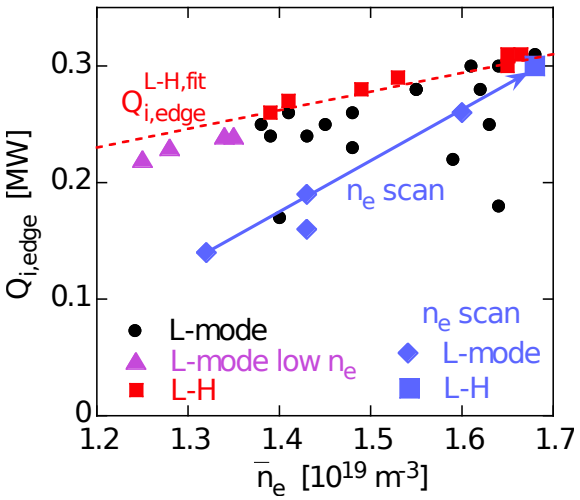

Figure 2: *L-modes and L-H transitions at 1MA: $Q_{i,edge}$ versus $\bar{n}_e$ for various P_{ECRH} and $\bar{n}_e$ values.*

the L-H transition, independently of T_e and P_{ECRH}. This shows experimentally that, below a given density, the H-mode cannot be achieved with pure electron heating.

3. L-H transitions with NBI

The key role of $Q_{i,edge}$ can be confirmed experimentally using, instead of ECRH, NBI at low acceleration voltage which provides a significant fraction of direct ion heating. Such experiments have been carried out at $\bar{n}_e \approx 1.75 \times 10^{19}\mathrm{m}^{-3}$, whereby the NBI has been increased in steps up the L-H transition, in some cases a constant P_{ECRH} was also applied with a maximum power of 0.7 MW.

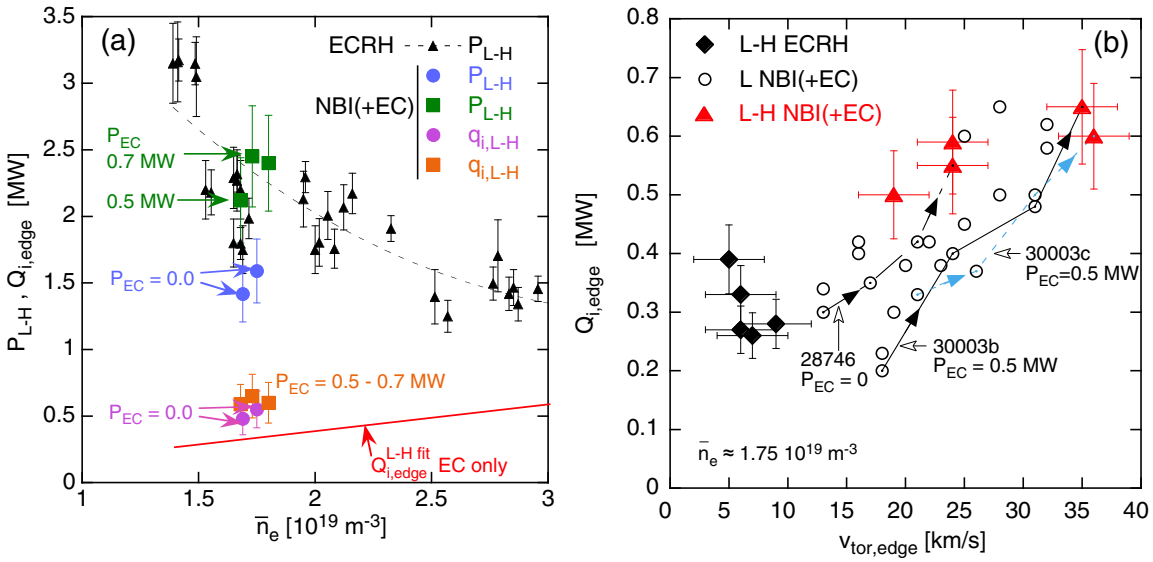

Figure 3: *Comparison of L-H transitions with NBI and ECRH at 1 MA: Panel (a):Power threshold and edge ion heat flux versus line-averaged density at the L-H transition including the NBI points. P_{EC} indicated the ECRH power added to NBI. Panel (b): $Q_{i,edge}$ versus $v_{tor,edge}$.*

The results, plotted in figure 3 (a), indicate that with NBI only P_{L-H} is indeed lower than with ECRH at the same density. Adding ECRH to NBI increases P_{L-H} by P_{ECRH} showing that electron heating does not contribute to achieving the L-H transition under these conditions. The power balance analysis reveals that this is due to the fact that the direct ion heating from NBI dominates and that the p_{ei} contribution is negligible. This is confirmed by the fact that $Q^{L-H}_{i,edge}$ takes the same values within the experimental uncertainties, independently of P_{ECRH}. However, $Q^{L-H}_{i,edge}$ with NBI is about two times larger than for the cases with ECRH only. This can be explained by the increase of P_{L-H} with the edge toroidal rotation ($v_{tor,edge}$) reported for DIII-D, [15]. This is illustrated by figure 3 (b) in which $Q_{i,edge}$ is plotted versus $v_{tor,edge}$ for L-mode and L-H points at $\bar{n}_e \approx 1.75 \times 10^{19}\mathrm{m}^{-3}$. The lowest $Q^{L-H}_{i,edge}$ values are obtained at the lowest rotation with ECRH only. As NBI is increased, both $Q^{L-H}_{i,edge}$ and $v_{tor,edge}$ increase, as illustrated by the trajectories of three NBI-heated discharges indicated by arrows. This plot demonstrates clearly that the L-H transition results from a competition between $Q^{L-H}_{i,edge}$ and $v_{tor,edge}$ as the NBI power is increased. This effect is attributed to the impact of $v_{tor,edge}$ on the E_r profile, which, however, cannot be investigated quantitatively with the present data.

4. Minimum threshold density and prediction for other devices

The above results suggest that the increase of P_{L-H} towards low densities is caused by the decoupling of the electron and ion heat channels such that the energy exchange is not complete at the edge and $Q_{i,edge}$ decreases despite the higher heating power. The global electron-ion energy transfer depends on τ_E/τ_{ei} where τ_E is the energy confinement time and τ_{ei} the volume-averaged electron-ion energy exchange time. Indeed we find in ASDEX Upgrade that $n_{e,min}$ occurs at $\tau_E/\tau_{ei} \approx 9$ at both 1MA and 0.6MA. This condition can be re-written in terms of control parameters combining the L-mode confinement and threshold scalings, for the values at the L-H transition, yielding: $n_{e,min}^{scal} \approx 0.7 I_p^{0.34} B_T^{0.62} a^{-0.95} (R/a)^{0.4}$, where a is the minor radius. As shown in figure 4, this formula reproduces well the experimental $n_{e,min}$ values in several tokamaks, in particular the high value in Alcator C-Mod which results from high I_p and B_T combined with the small machine size. Applying $n_{e,min}^{scal}$ to ITER yields: $n_{e,min} \approx 4 \times 10^{19} \mathrm{m}^{-3}$ and $P_{L-H} \approx 42$ MW at full field and current, while they decrease to $n_{e,min} \approx 2.2 \times 10^{19} \mathrm{m}^{-3}$ and $P_{L-H} \approx 16$ MW at half field and current. The latter, an option for the non-nuclear phase, seems to be reachable with ECRH only.

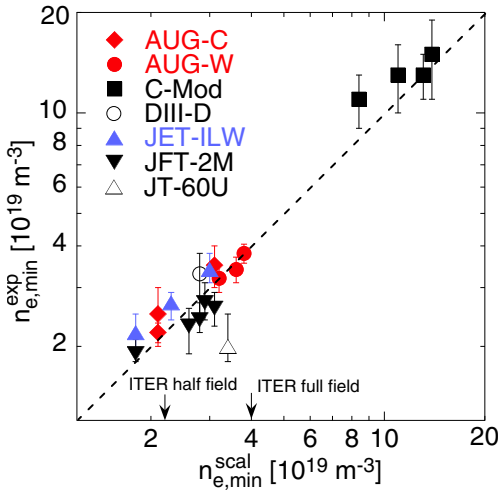

Figure 4: *Minimum threshold density: experimental values versus formula.*

References

[1] BIGLARI, H. et al., Phys. Fluids B **2** (1990) 1.
[2] GROEBNER, R. J. et al., Phys. Rev. Lett. **64** (1990) 3015.
[3] BURRELL, K. H., Phys. Plasmas **4** (1997) 1499.
[4] WAGNER, F., Plasma Physics and Controlled Fusion **49** (2007) B1.
[5] SAUTER, P. et al., Nuclear Fusion **52** (2012) 012001.
[6] HINTON, F. L. et al., Rev. Mod. Phys. **48** (1976) 239.
[7] MCDERMOTT, R. M. et al., Physics of Plasmas **16** (2009) 056103.
[8] STROTH, U. et al., Plasma Physics and Controlled Fusion **53** (2011) 024006.
[9] VIEZZER, E. et al., Nuclear Fusion **53** (2013) 053005.
[10] RYTER, F. et al., Nuclear Fusion **54** (2014) 083003.
[11] PANKIN, A. et al., Computer Phys. Comm. **159** (2004) 157.
[12] MCDERMOTT, R. M. et al., Plasma Physics and Controlled Fusion **53** (2011) 124013.
[13] RYTER, F. et al., Nuclear Fusion **49** (2009) 062003.
[14] RYTER, F. et al., Nuclear Fusion **53** (2013) 113003.
[15] GOHIL, P. et al., Nuclear Fusion **50** (2010) 064011.